Electronic Supplementary Information (ESI) for

Unsymmetrical β-Functionalized 'Push-Pull' Porphyrins: Synthesis, Photophysical, Electrochemical and Nonlinear Optical Properties

Pinki Rathi,[a] Ekta,[a] Sandeep Kumar,[a] Dipanjan Banerjee,[b] Soma Venugopal Rao[b*] Muniappan Sankar[a*]

[a]Department of Chemistry, Indian Institute of Technology Roorkee, Roorkee 247667, India

[b]Advanced Centre of Research in High Energy Materials (ACRHEM), University of Hyderabad, Hyderabad 500046, Telangana, India

Table of contents

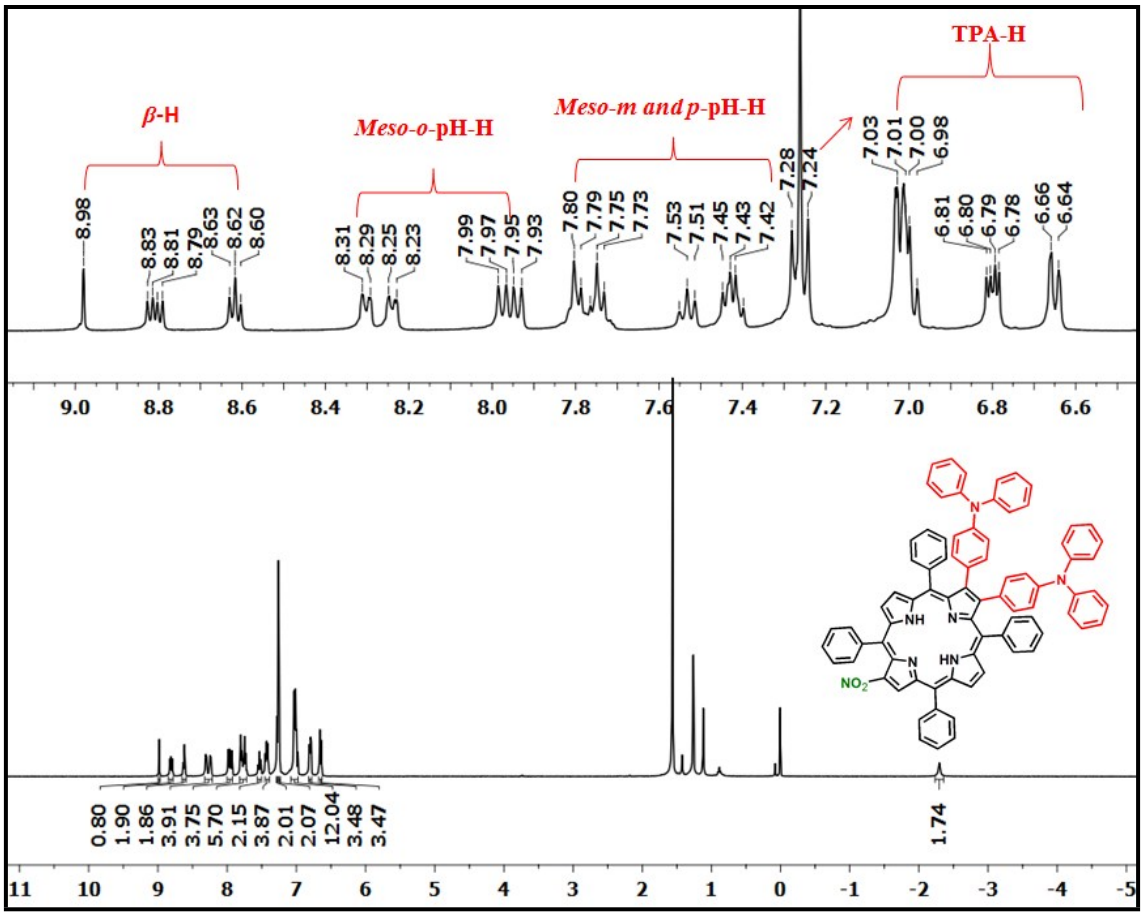

Figure S1. ^{1}H NMR spectrum of $H_2TPP(TPA)_2NO_2$ in $CDCl_3$ at 298 K.

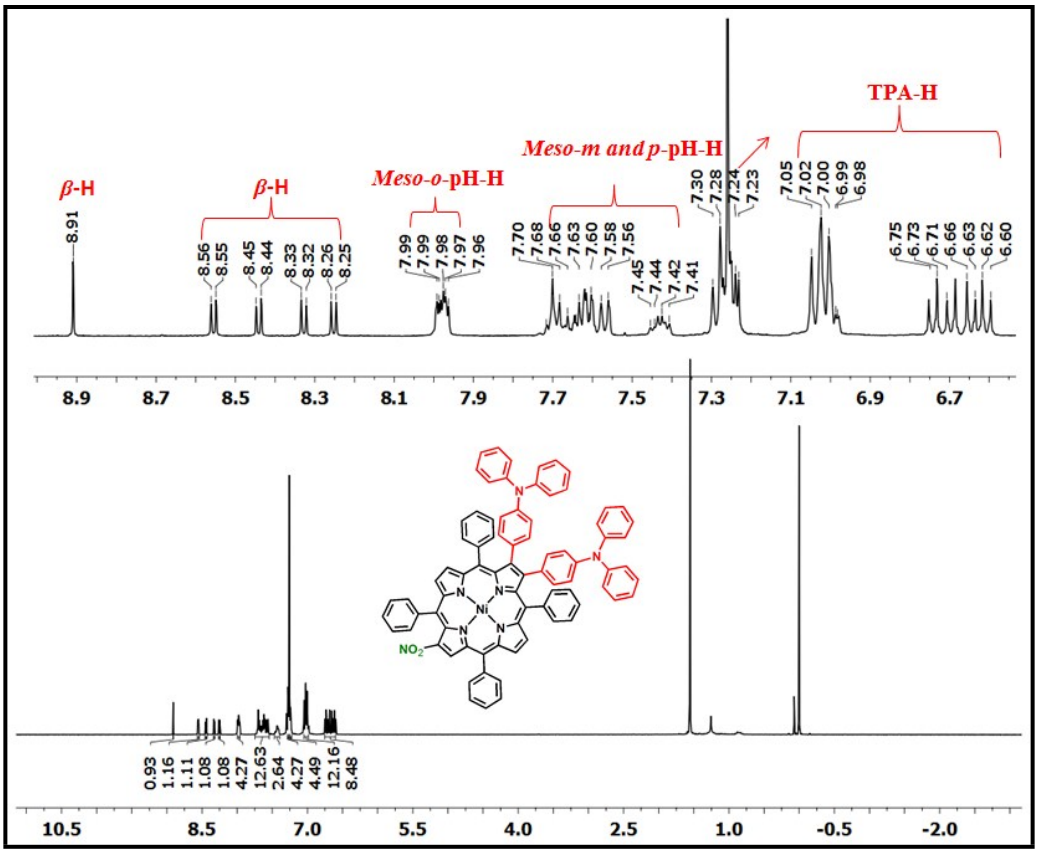

Figure S2. ^{1}H NMR spectrum of NiTPP(TPA)$_2$NO$_2$ in CDCl$_3$ at 298 K.

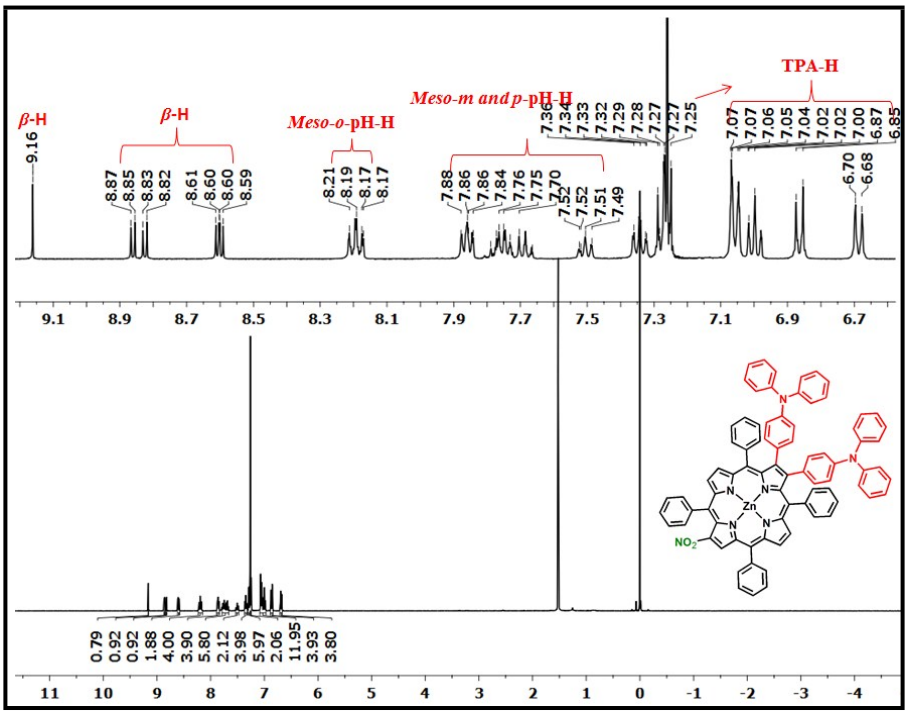

Figure S3. ^{1}H NMR spectrum of ZnTPP(TPA)$_2$NO$_2$ in CDCl$_3$ at 298 K.

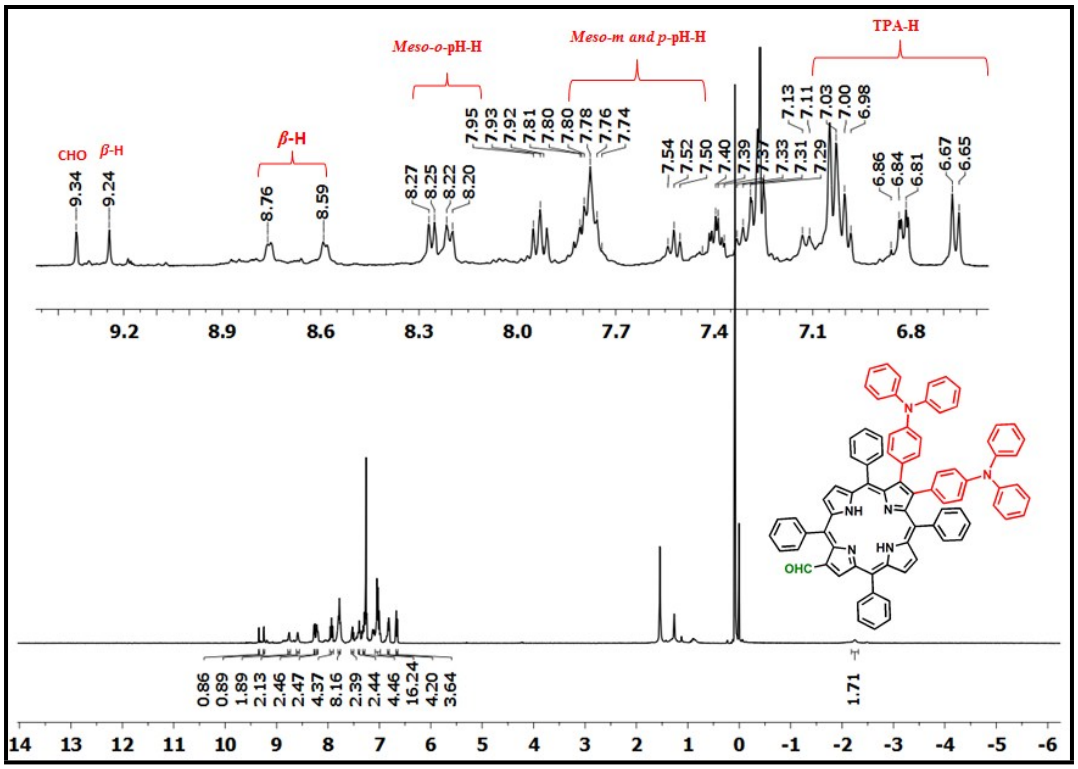

Figure S4. ^{1}H NMR spectrum of $H_2TPP(TPA)_2CHO$ in $CDCl_3$ at 298 K.

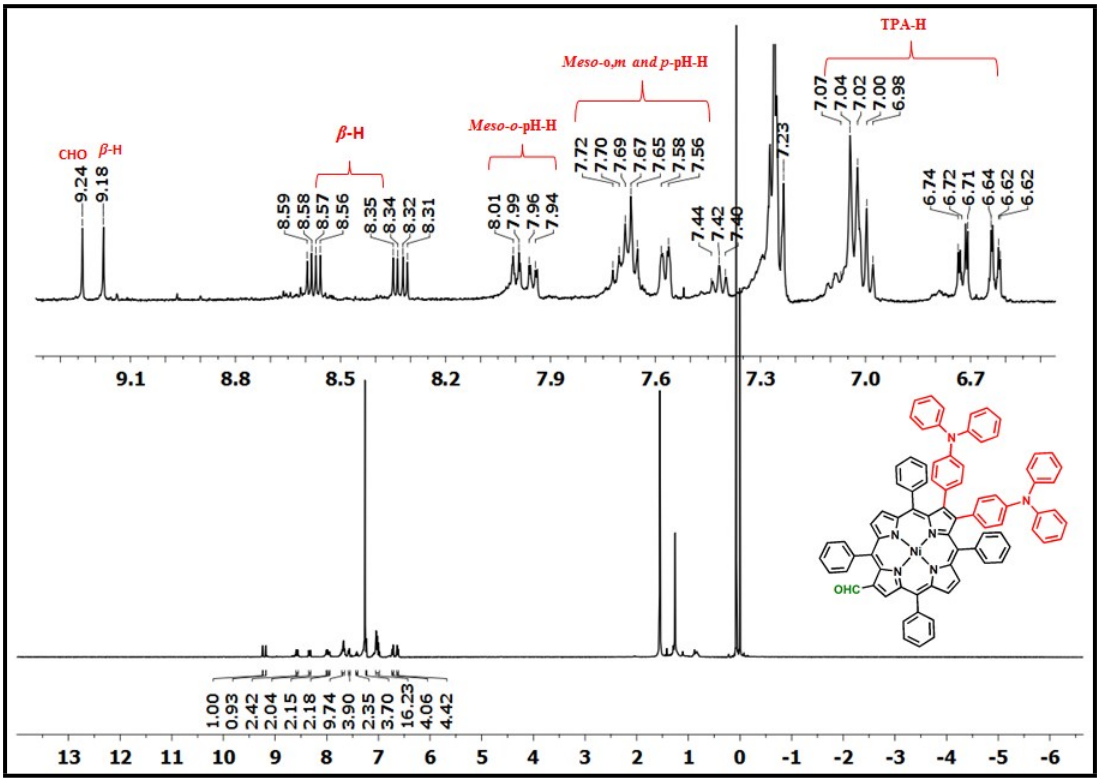

Figure S5. ^{1}H NMR spectrum of $NiTPP(TPA)_2CHO$ in $CDCl_3$ at 298 K.

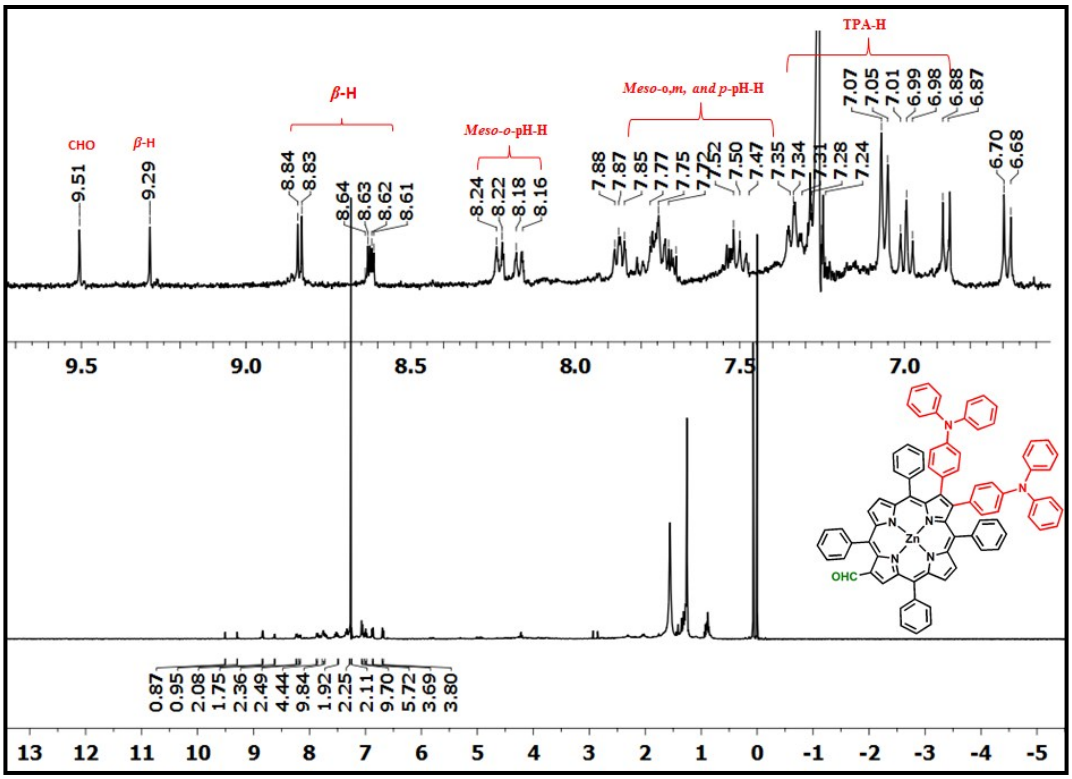

Figure S6. ^{1}H NMR spectrum of ZnTPP(TPA)$_2$CHO in CDCl$_3$ at 298 K.

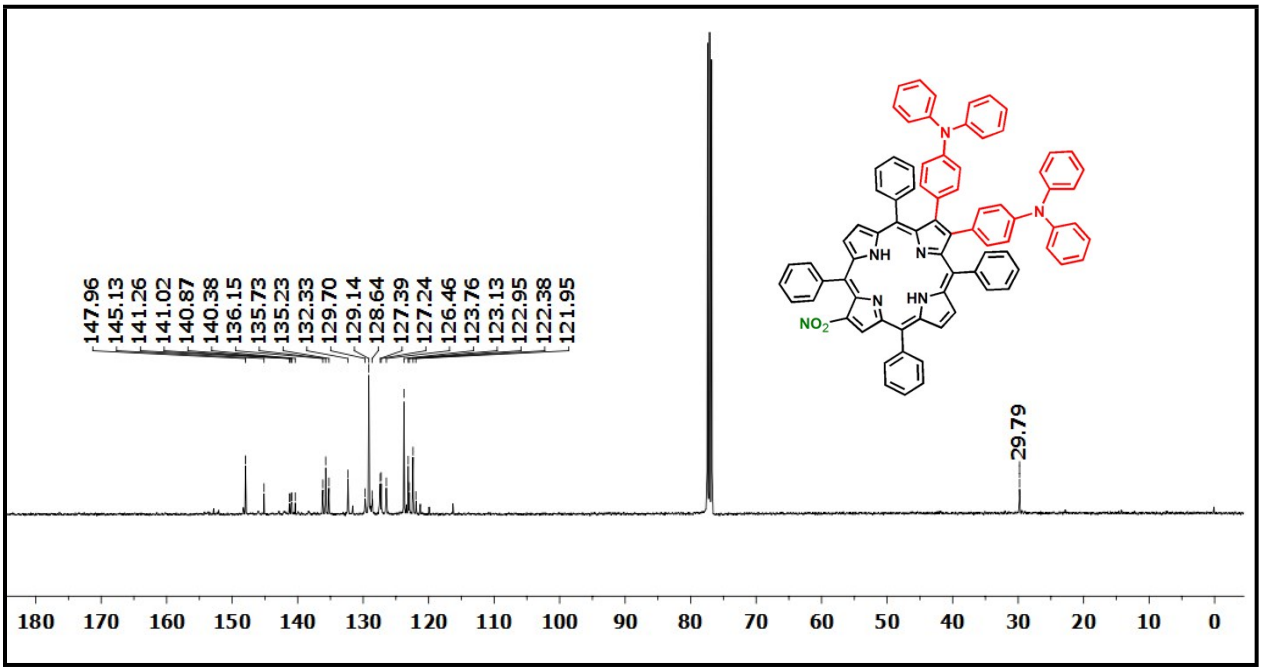

Figure S7. ^{13}C NMR spectrum of H$_2$TPP(TPA)$_2$NO$_2$ in CDCl$_3$ at 298 K

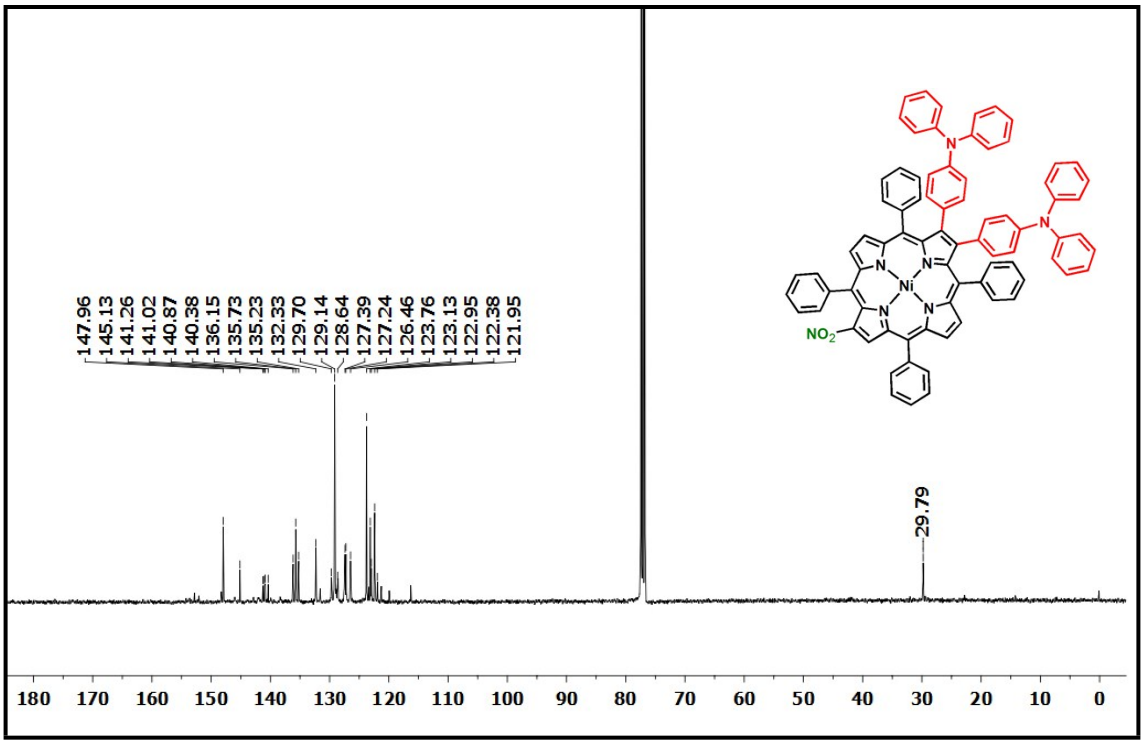

Figure S8. ^{13}C NMR spectrum of NiTPP(TPA)$_2$NO$_2$ in CDCl$_3$ at 298 K

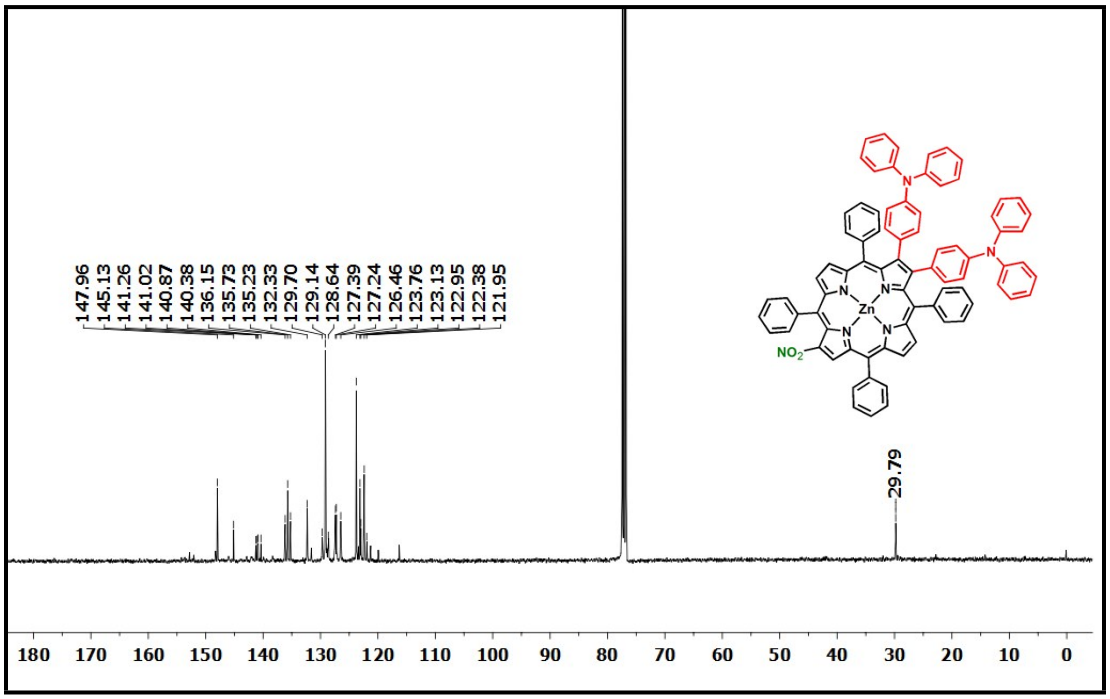

Figure S9. ^{13}C NMR spectrum of ZnTPP(TPA)$_2$NO$_2$ in CDCl$_3$ at 298 K

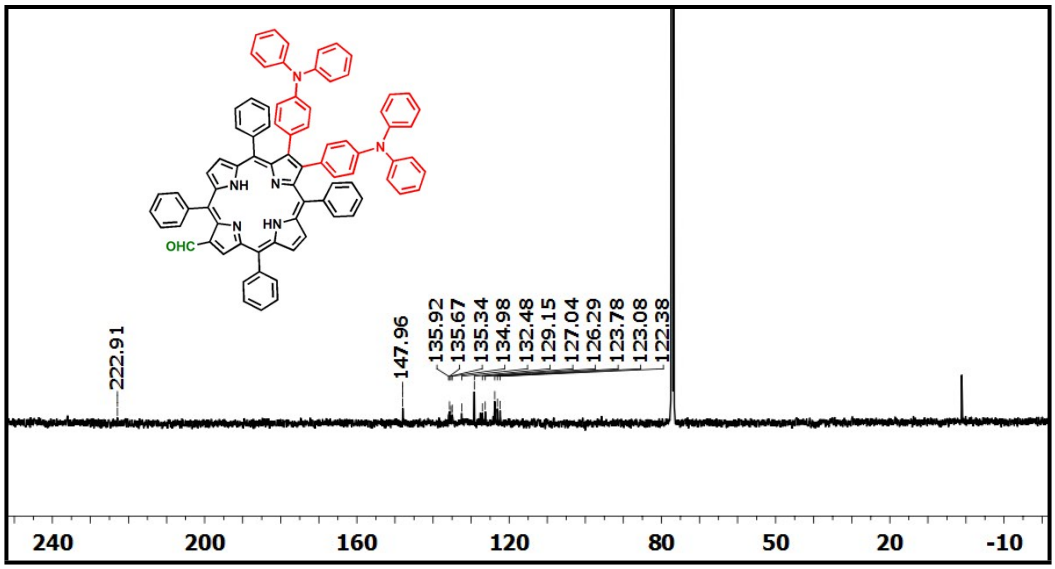

Figure S10. ^{13}C NMR spectrum of $H_2TPP(TPA)_2CHO$ in $CDCl_3$ at 298 K

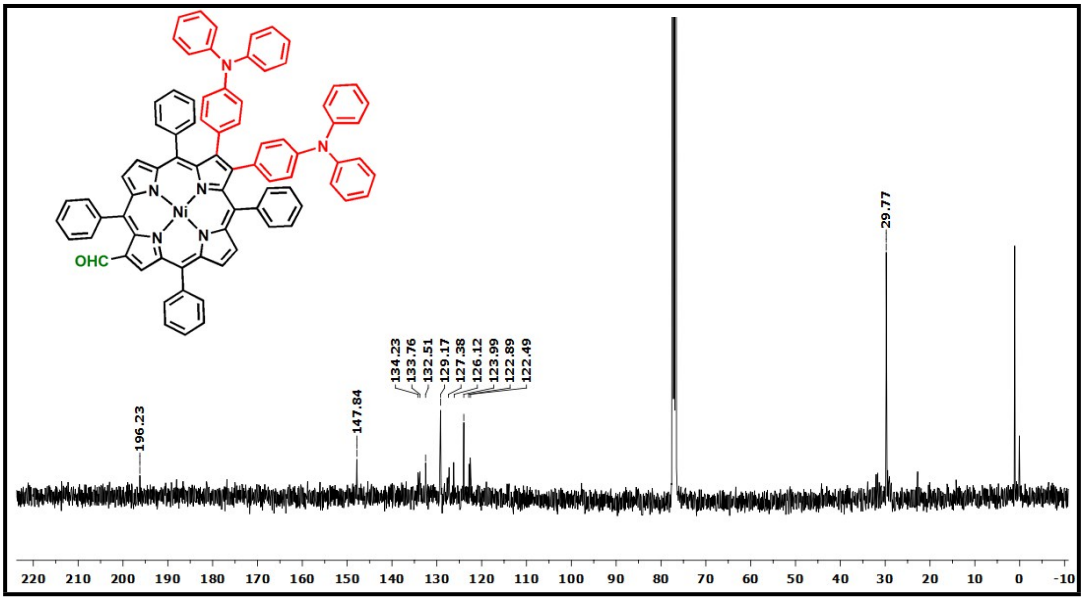

Figure S11. ^{13}C NMR spectrum of $NiTPP(TPA)_2CHO$ in $CDCl_3$ at 298 K

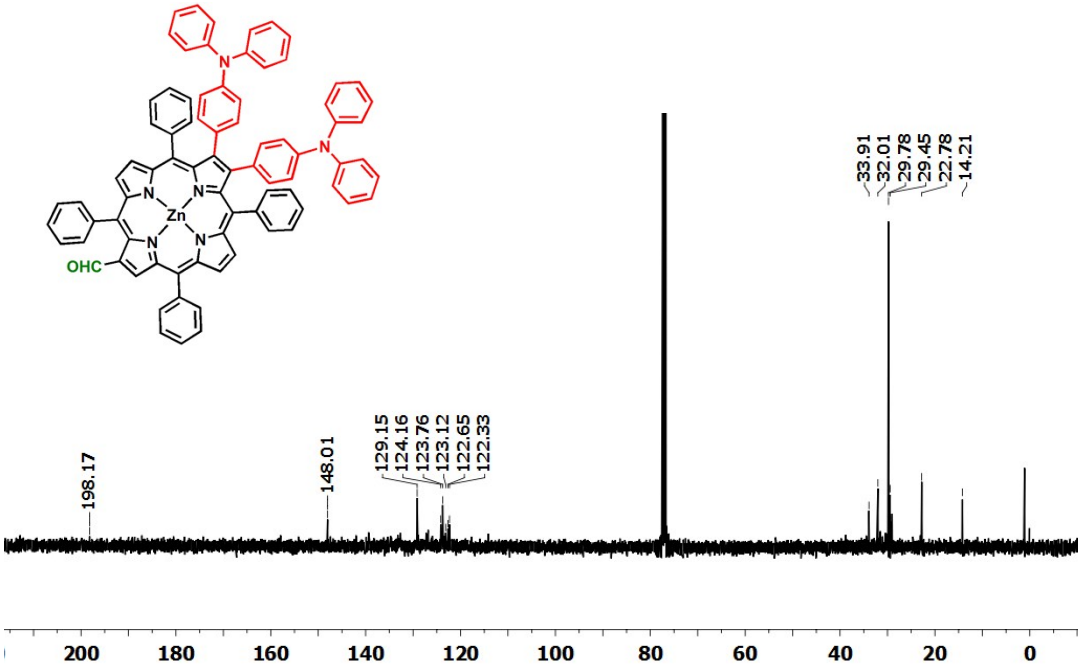

Figure S12. ^{13}C NMR spectrum of $ZnTPP(TPA)_2CHO$ in $CDCl_3$ at 298 K

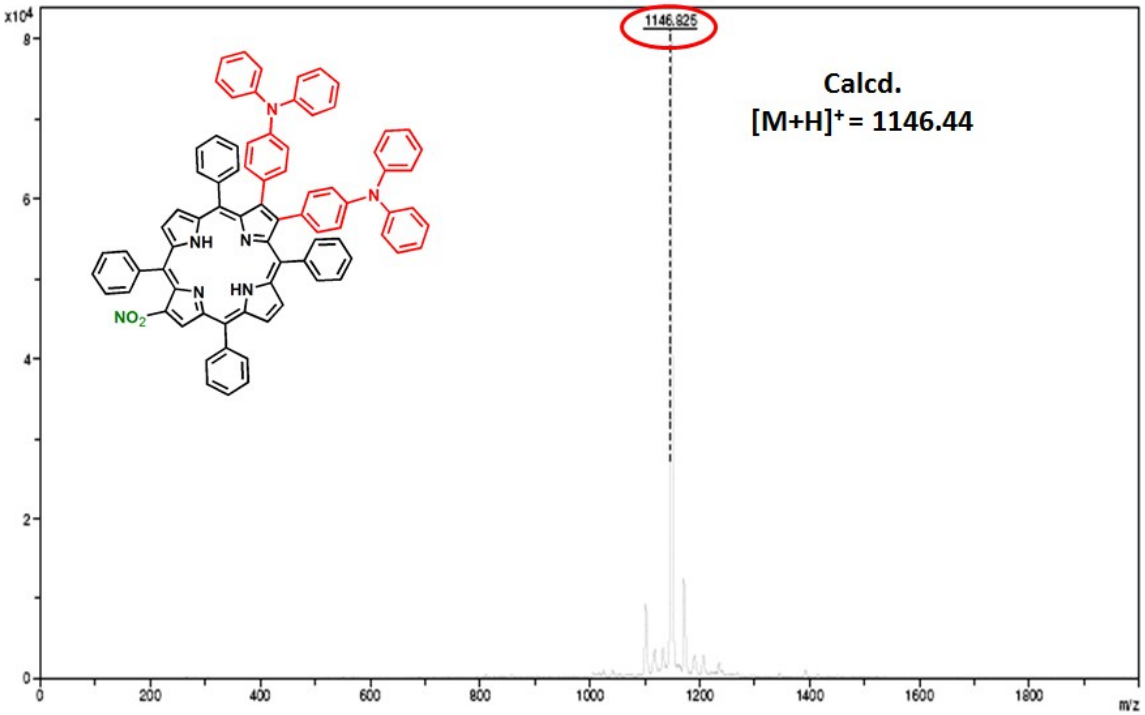

Figure S13. MALDI-TOF mass spectrum of $H_2TPP(TPA)_2NO_2$.

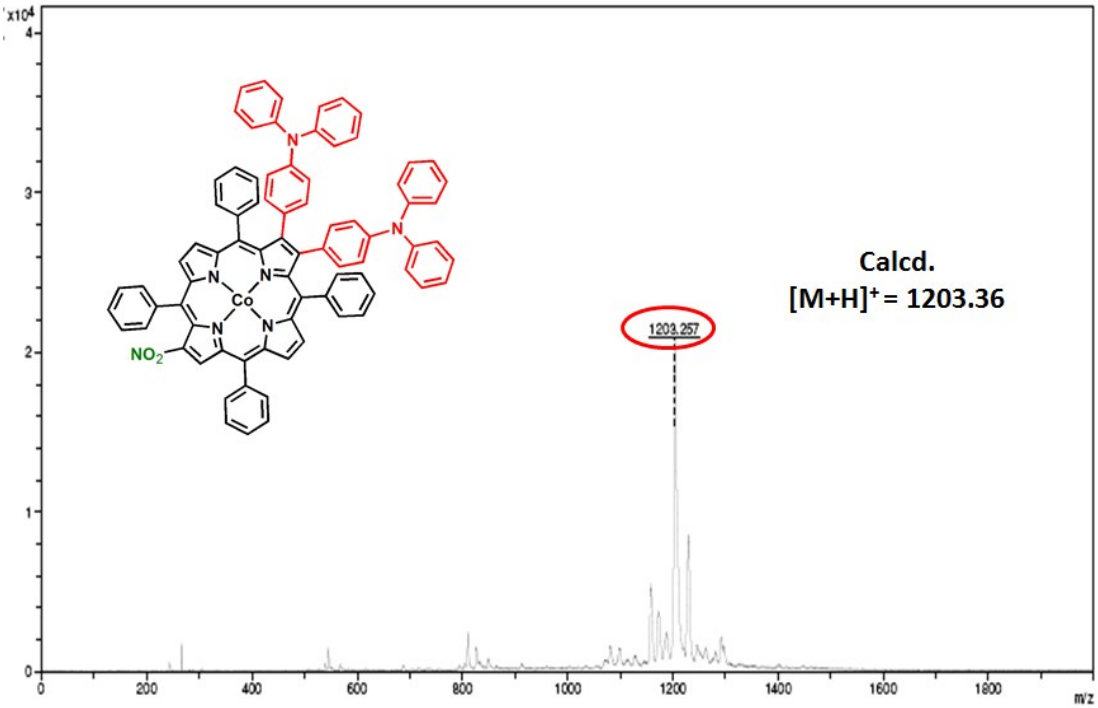

Figure S14. MALDI-TOF mass spectrum of CoTPP(TPA)$_2$NO$_2$.

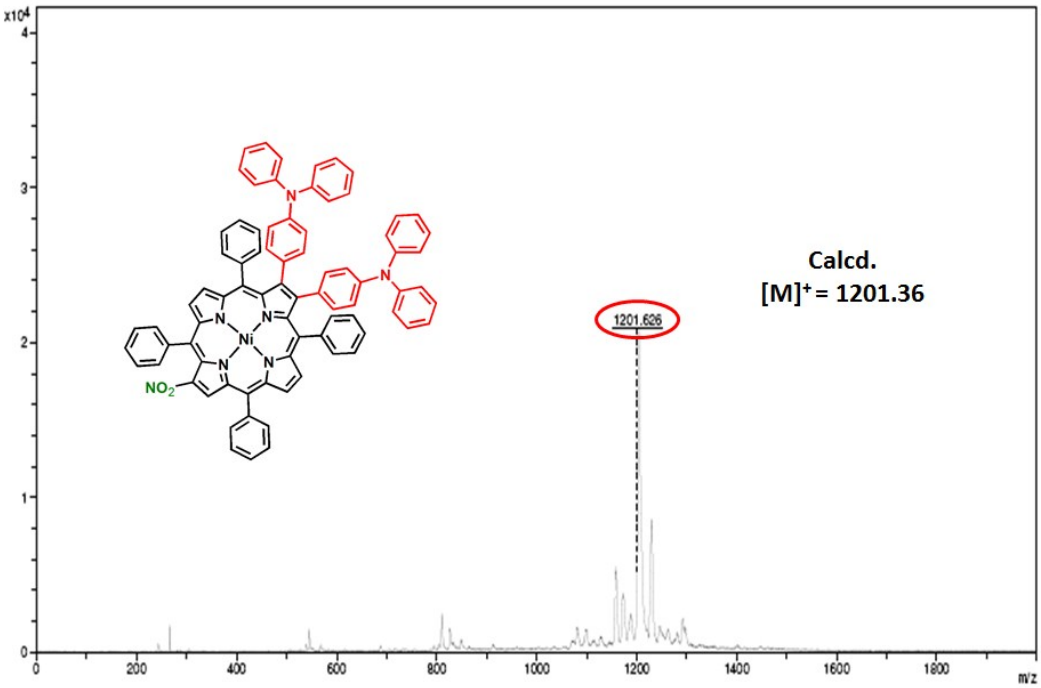

Figure S15. MALDI-TOF mass spectrum of NiTPP(TPA)$_2$NO$_2$.

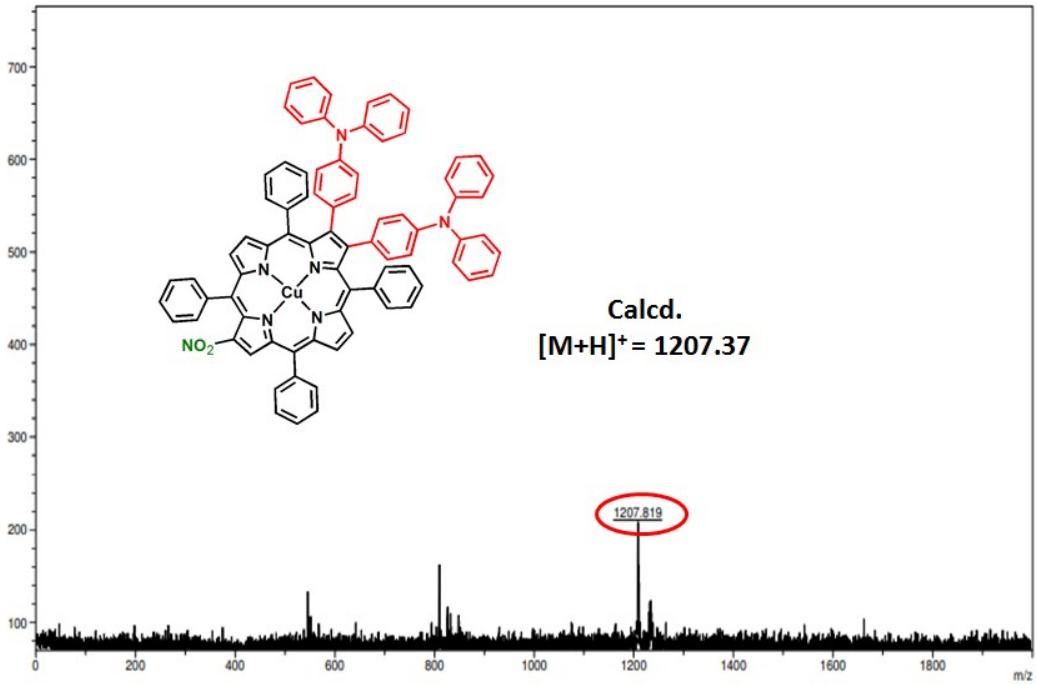

Figure S16. MALDI-TOF mass spectrum of CuTPP(TPA)$_2$NO$_2$.

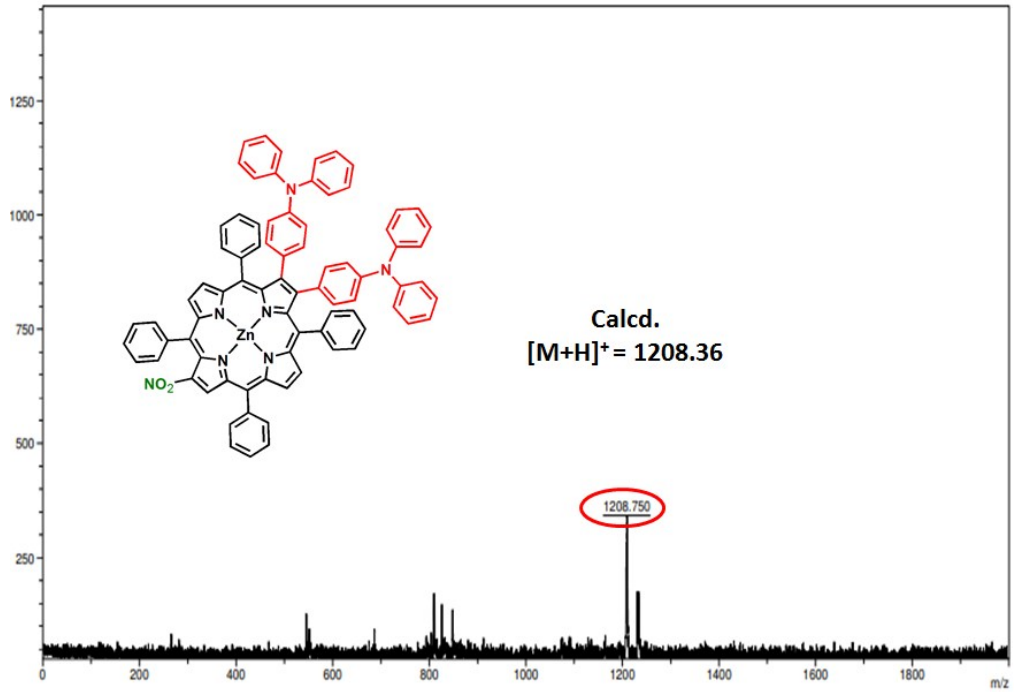

Figure S17. MALDI-TOF mass spectrum of ZnTPP(TPA)$_2$NO$_2$.

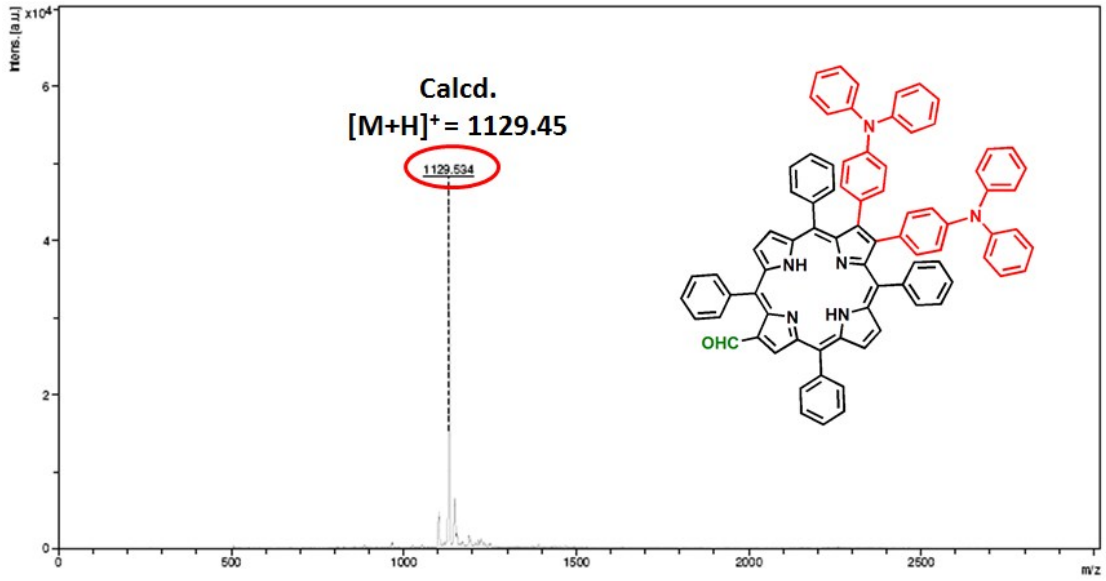

Figure S18. MALDI-TOF mass spectrum of $H_2TPP(TPA)_2CHO$.

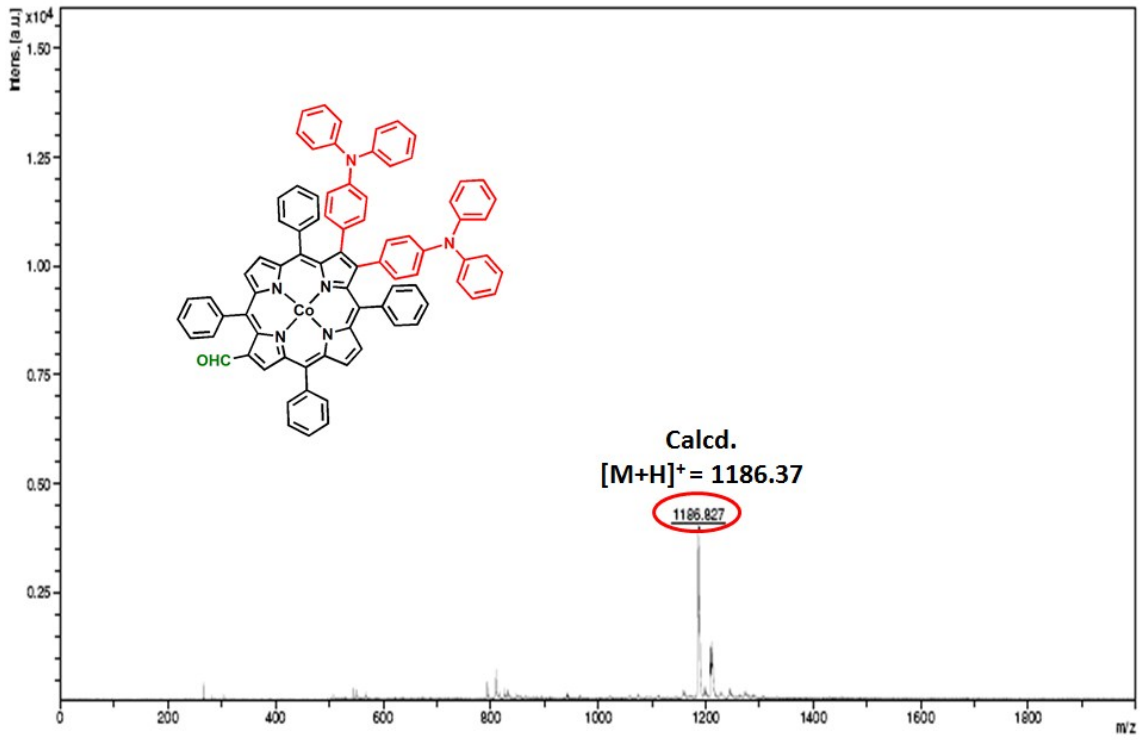

Figure S19. MALDI-TOF mass spectrum of $CoTPP(TPA)_2CHO$.

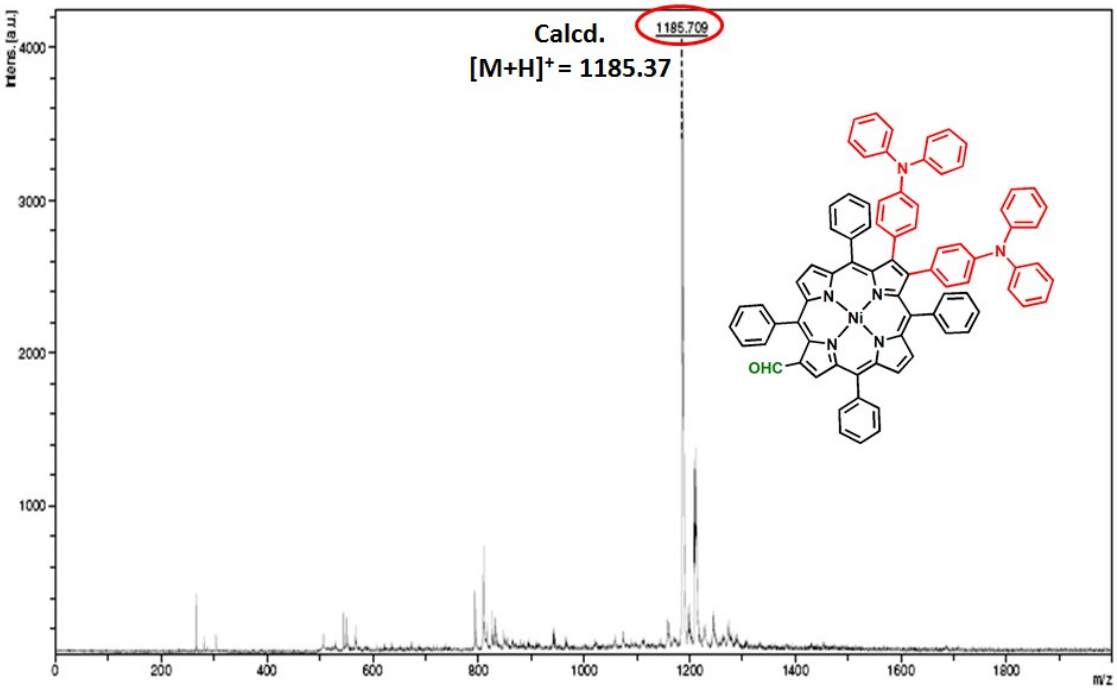

Figure S20. MALDI-TOF mass spectrum of NiTPP(TPA)$_2$CHO.

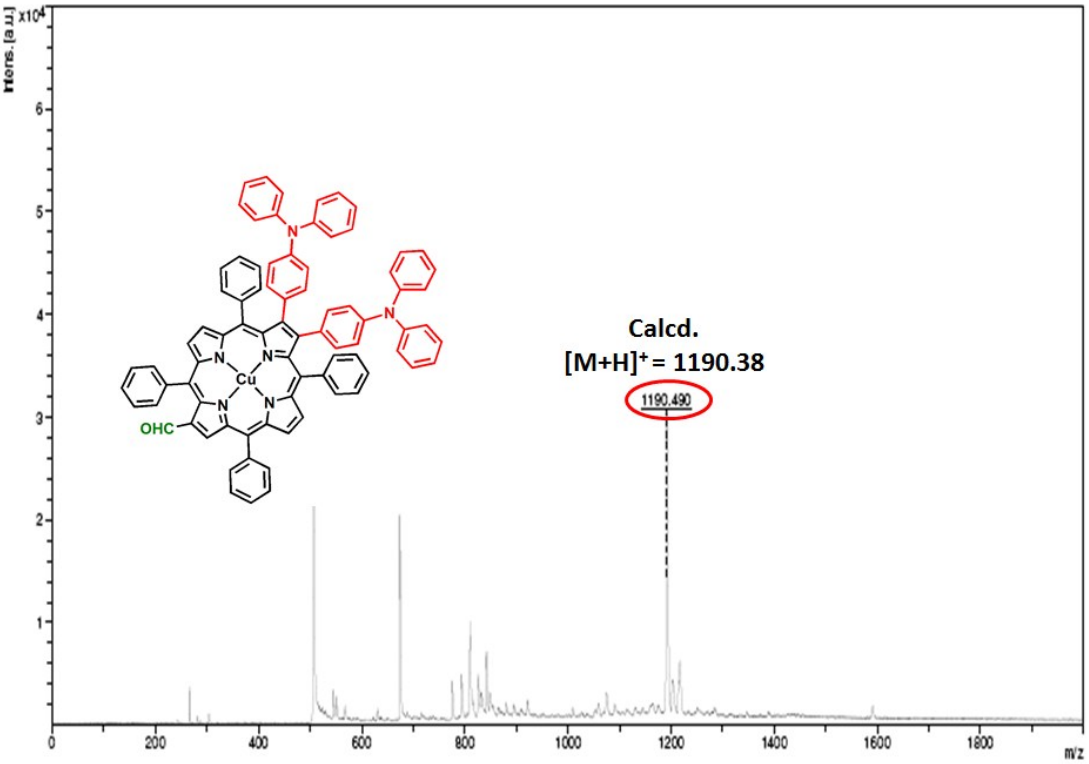

Figure S21. MALDI-TOF mass spectrum of CuTPP(TPA)$_2$CHO.

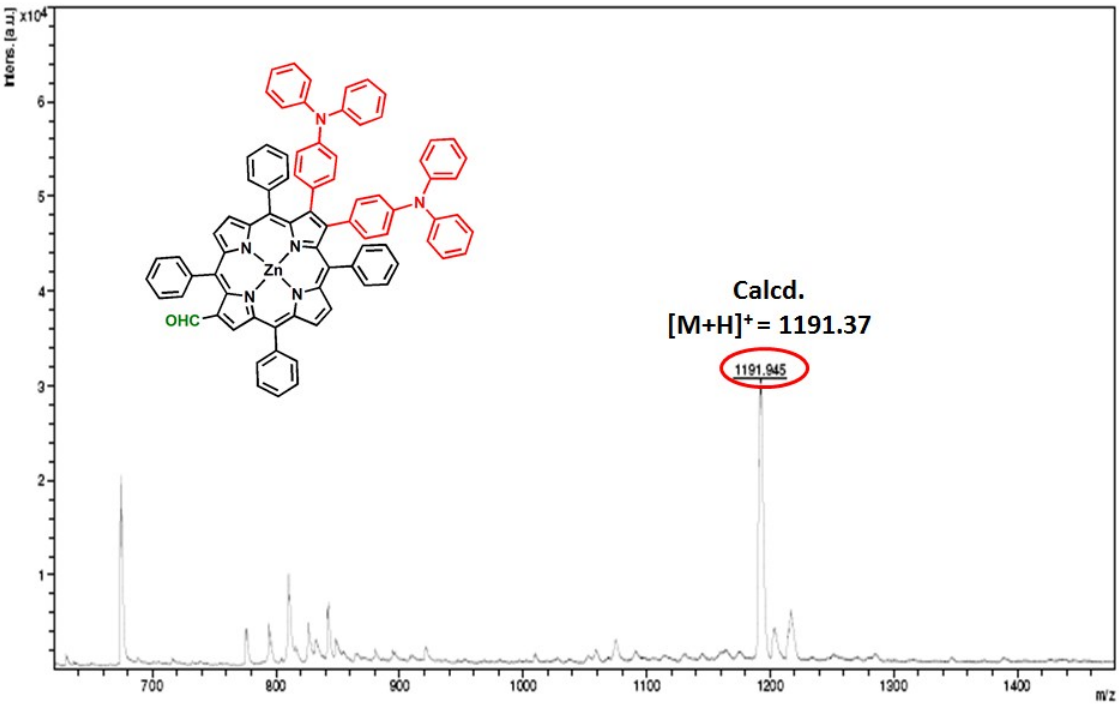

Figure S22. MALDI-TOF mass spectrum of ZnTPP(TPA)$_2$CHO.

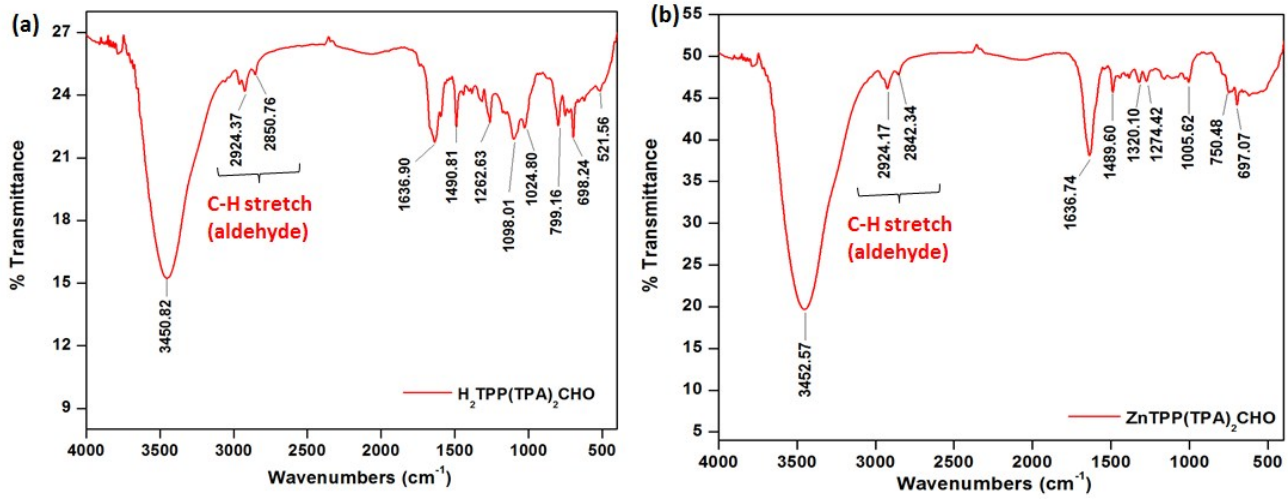

Figure S23. IR spectra of (a) $H_2TPP(TPA)_2CHO$ and (b) $ZnTPP(TPA)_2CHO$.

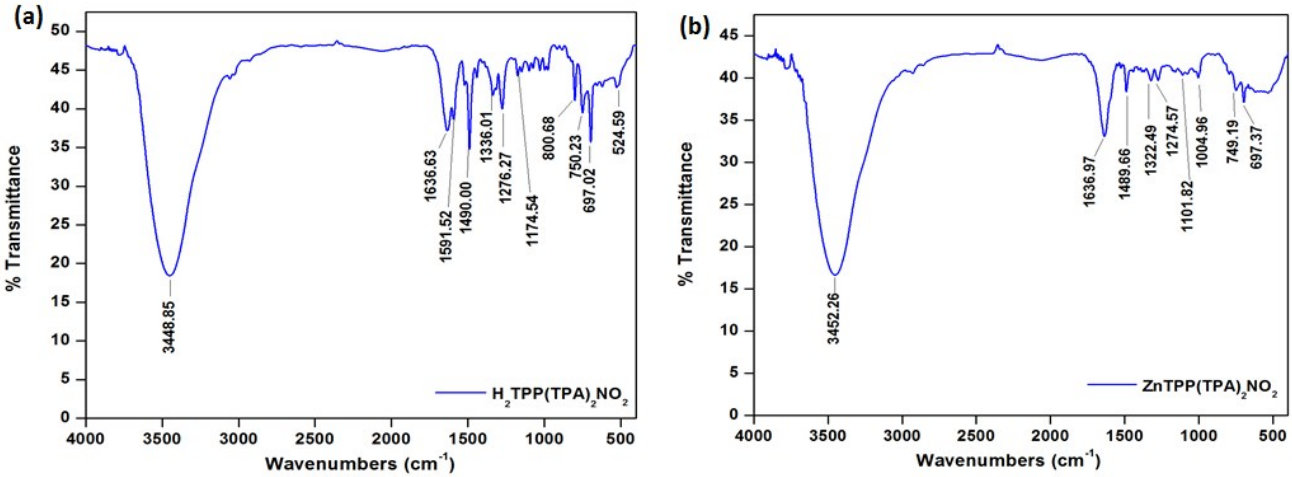

Figure S24. IR spectra of (a) $H_2TPP(TPA)_2NO_2$ and (b) $ZnTPP(TPA)_2NO_2$.

Table S1. Photophysical data of $MTPP(TPA)_2NO_2$ and $MTPP(TPA)_2CHO$ (2H, Co^{II}, Ni^{II}, Cu^{II}, Zn^{II}) in CH_2Cl_2 at 298 K

Porphyrin	$\lambda_{excitation}$, nm	$\lambda_{emission}$, nm	Φ_f	FWHM	τ [ns]
$H_2TPP(TPA)_2NO_2$	308(4.65), 438(5.13), 539(4.12), 690(3.83)	754	0.0019	40	0.52
$H_2TPP(TPA)_2CHO$	308(4.69), 438(5.24), 535(4.06), 576(3.88), 612(3.72), 678(3.61)	701	0.019	29	4.88
$CoTPP(TPA)_2NO_2$	308(4.76), 432(5.01), 551(4.11), 597(4.10)			60	
$CoTPP(TPA)_2CHO$	308(4.70), 434(5.11), 555(4.16), 593(4.09)			45	
$NiTPP(TPA)_2NO_2$	309(4.77), 438(5.11), 553(4.17), 602(4.14)			44	
$NiTPP(TPA)_2CHO$	309(4.76), 437(5.34), 554(4.11), 598(4.08)			32	
$CuTPP(TPA)_2NO_2$	309(4.73), 432(5.17), 559(4.16), 606(4.10)			41	
$CuTPP(TPA)_2CHO$	309(4.81), 434(5.46), 559(4.25), 600(4.20)			25	
$ZnTPP(TPA)_2NO_2$	309(4.85), 434(5.50), 560(4.47), 609(4.36)	698	0.003	37	0.58
$ZnTPP(TPA)_2CHO$	311(4.42), 434(5.16), 562(3.91), 603(3.83)	647	0.009	23	0.89

Table S2. Redox Potential Data of all Synthesized Porphyrins with Comparative Porphyrins containing 0.1 M $TBAPF_6$ with scan rate 0.1 Vs^{-1} at 298K.

Porphyrin	Oxidation				ΔE (V)	Reduction			$M^{II/III}$	$M^{II/I}$
	I	II	III	IV		I	II	III		
H_2TPP	1.00	1.34			2.23	-1.23	-1.54			
$H_2TPPBr_2NO_2$	1.11	1.21			1.87	-0.75	-0.82			
$H_2TPP(TPA)_2NO_2$	1.02	1.62			1.85	-0.83	-0.98			
H_2TPPBr_2CHO	1.11	1.22			2.00	-0.89				
$H_2TPP(TPA)_2CHO$	1.10				2.05	-0.94				
CoTPP	1.06	1.31			2.44	-1.38			0.85	-0.86
$CoTPPBr_2NO_2$	1.22	1.44			2.43	-1.20			0.92	-0.51
$CoTPP(TPA)_2NO_2$	1.22	1.51			2.47	-1.25			0.96	-0.60
$CoTPPBr_2CHO$	1.26	1.41			2.28	-1.02	-1.49		0.95	-0.57
$CoTPP(TPA)_2CHO$	1.23	1.45			2.36	-1.13			0.98	-0.67
NiTPP	1.02	1.32			2.30	-1.28	-1.72			
$NiTPPBr_2NO_2$	1.24				2.07	-0.83	-1.06			
$NiTPP(TPA)_2NO_2$	0.95	1.23			1.82	-0.87	-1.14	-1.4		
$NiTPPBr_2CHO$	1.14				2.09	-0.95	-1.21			
$NiTPP(TPA)_2CHO$	1.03	1.26	1.5	2.0	2.09	-1.05	-1.05			
CuTPP	0.97	1.35			2.30	-1.33	-1.70			
$CuTPPBr_2NO_2$	1.07	1.49			1.92	-0.85	-1.07			
$CuTPP(TPA)_2NO_2$	1.00	1.50			1.89	-0.89	-1.14	-1.3		
$CuTPPBr_2CHO$	1.08	1.47			2.02	-0.94	-1.20			
$CuTPP(TPA)_2CHO$	1.06	1.47			2.03	-0.97	-1.34			
ZnTPP	0.84	1.15			2.20	-1.36	-1.77			
$ZnTPPBr_2NO_2$	0.94	1.18			1.88	-0.93	-1.08			
$ZnTPP(TPA)_2NO_2$	0.98	1.23			2.05	-1.07	-1.30			
$ZnTPPBr_2CHO$	0.97	1.22			2.02	-1.05	-1.20			
$ZnTPP(TPA)_2CHO$	1.04	1.55			2.16	-1.11	-1.36			

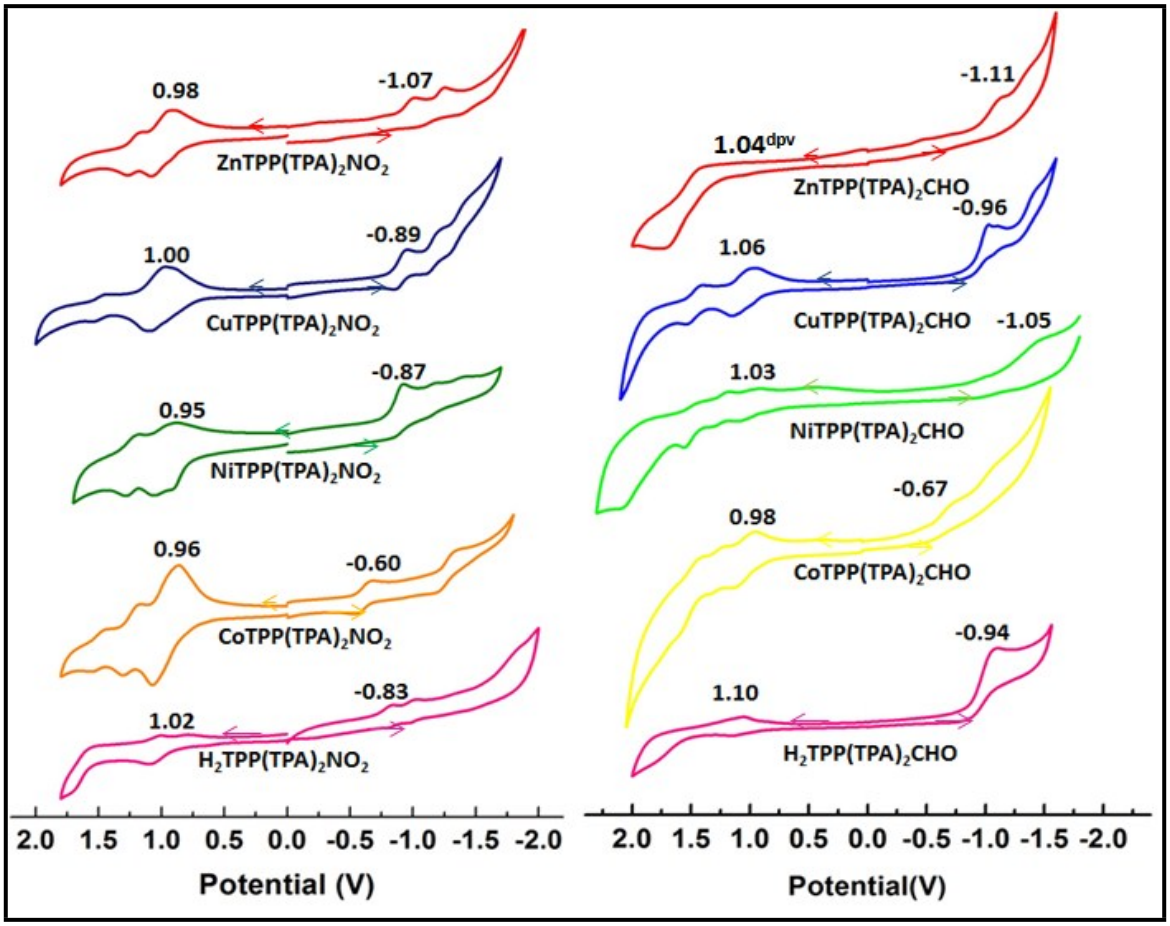

Figure S25. Cyclic Voltammograms of Porphyrins (a) $MTPP(TPA)_2NO_2$ and $MTPP(TPA)_2CHO$ (M = 2H, Co(II), Cu(II), Ni(II), Zn(II)) and in CH_2Cl_2 with a Scan Rate of 0.1 V/s at 298 K.

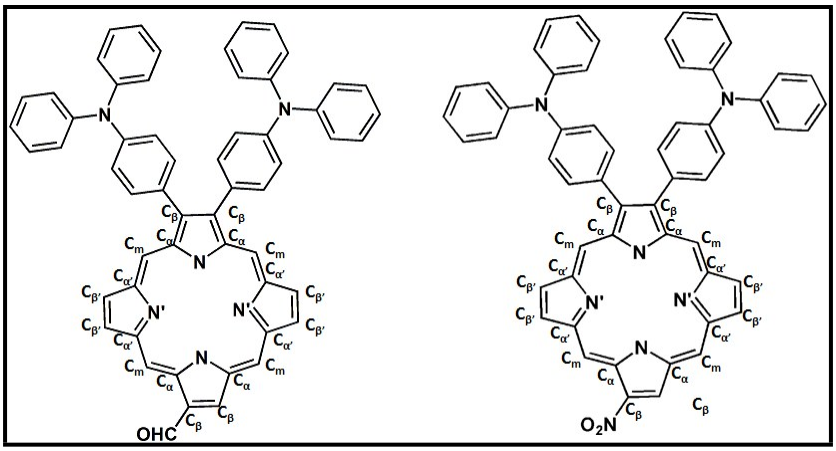

Table S3. Selected Average Bond Lengths (Å) and Bond Angles (°) for the B3LYP/LANL2DZ Optimized Geometry of $H_2TPP(TPA)_2NO_2/CHO$ and $ZnTPP(TPA)_2NO_2/CHO$.

	H_2TPPBr_2CHO	**$H_2TPP(TPA)_2CHO$**	**$H_2TPPBr_2NO_2$**	**$H_2TPP(TPA)_2NO_2$**	**$ZnTPP(TPA)_2CHO$**	**$ZnTPP(TPA)_2NO_2$**
Bond Length (Å)						
M-N					2.080	2.090
M-N’					2.040	2.050
N-C_α	1.363	1.390	1.388	1.391	1.395	1.394
N′-$C_{\alpha'}$	1.375	1.390	1.392	1.390	1.396	1.395
C_α-C_β	1.462	1.450	1.460	1.440	1.462	1.459
$C_{\alpha'}$-$C_{\beta'}$	1.433	1.471	1.394	1.472	1.458	1.457
C_β-C_β	1.363	1.399	1.375	1.394	1.390	1.386
$C_{\beta'}$-$C_{\beta'}$	1.365	1.367	1.380	1.366	1.375	1.372
C_α-C_m	1.414	1.417	1.420	1.417	1.422	1.422
$C_{\alpha'}$-C_m	1.403	1.419	1.413	1.418	1.417	1.416
ΔC_β (Å)	**0.575**	**0.636**	**0.667**	**0.642**	**0.593**	**0.580**
Δ24 (Å)	**0.266**	**0.312**	**0.315**	**0.317**	**0.282**	**0.275**
ΔMetal (Å)					**0.011**	**0.033**
Bond Angle (deg)						
N-C_α-C_m	124.52	124.97	124.70	125.12	124.57	124.71
N′-$C_{\alpha'}$-C_m	127.19	126.37	127.00	126.33	126.40	126.26
N-C_α-C_β	109.91	106.33	109.20	110.28	108.91	108.81
N′-$C_{\alpha'}$-$C_{\beta'}$	106.29	110.26	106.40	106.11	108.86	108.95
C_β-C_α-C_m	125.47	123.33	125.90	123.34	126.41	126.45
$C_{\beta'}$-$C_{\alpha'}$-C_m	126.46	128.56	126.60	128.58	124.90	124.36
C_α-C_m-$C_{\alpha'}$	124.73	124.13	123.80	123.95	124.13	124.70
C_α-C_β-C_β	106.46	106.80	107.00	106.78	107.09	106.96
$C_{\alpha'}$-$C_{\beta'}$-$C_{\beta'}$	108.26	107.96	108.20	108.12	107.42	107.45
C_α-N- C_α	107.00	105.76	107.20	110.95	107.58	107.74
$C_{\alpha'}$-N′- $C_{\alpha'}$	110.83	111.11	110.60	110.73	107.30	107.22
M-N-C_α					125.18	125.27
M-N’-$C_{\alpha'}$					125.49	125.36
N-M-N					177.54	179.75
N’-M-N’					178.70	177.23

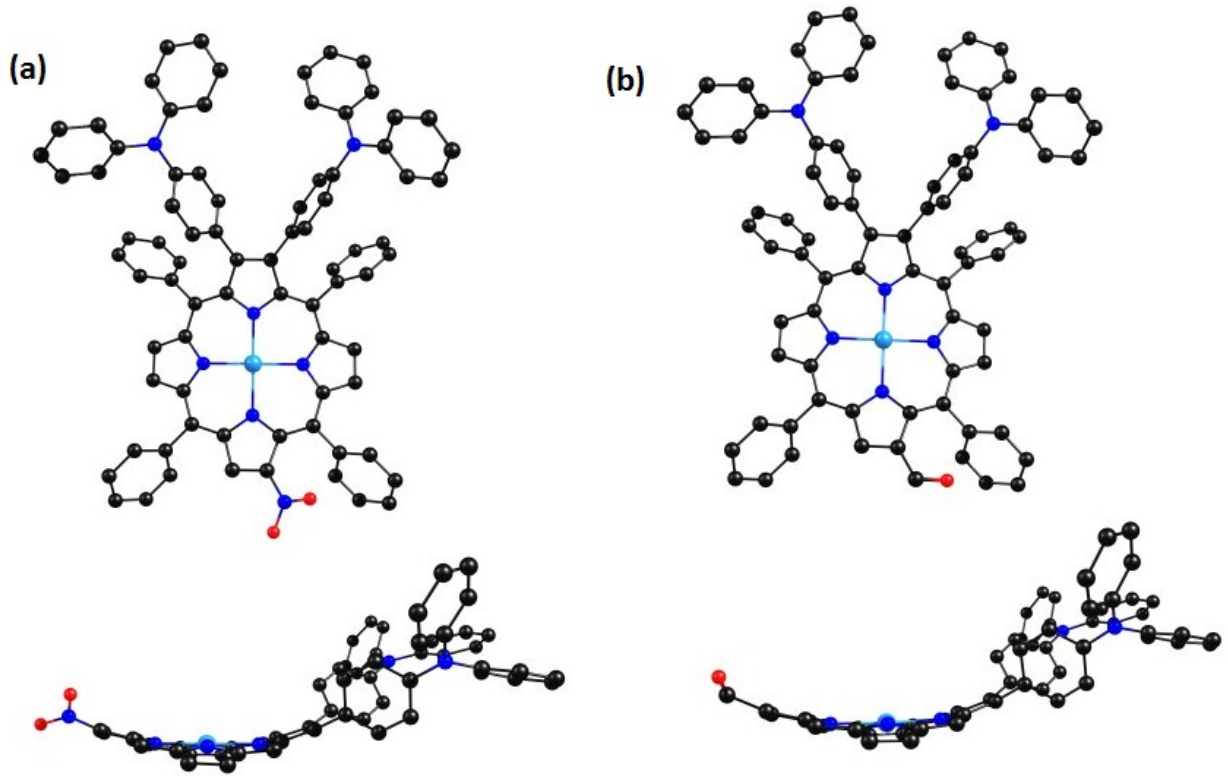

Figure S26. Optimized gas phase geometries of (a) $ZnTPP(TPA)_2NO_2$ and (b) $ZnTPP(TPA)_2CHO$.

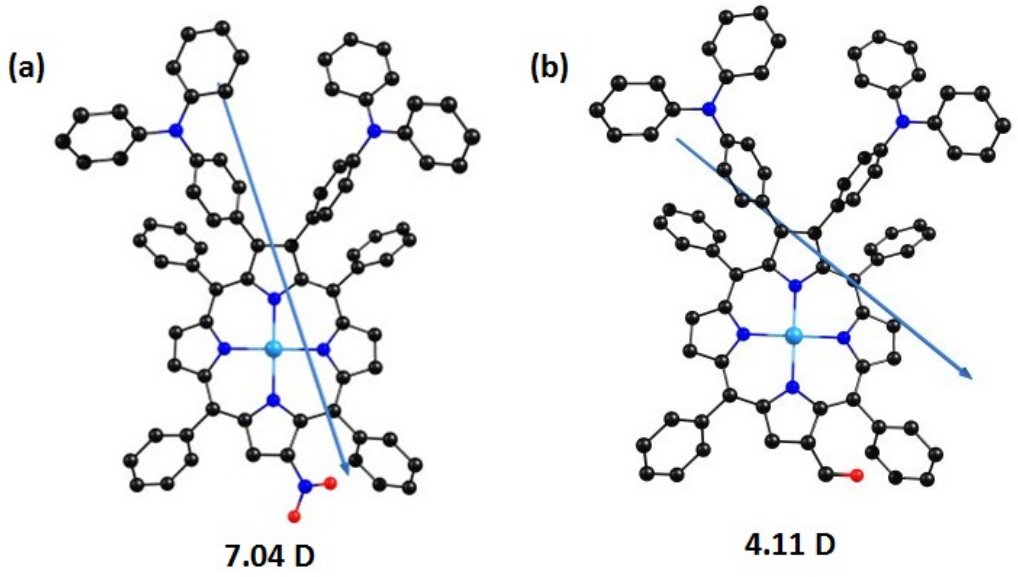

Figure S27. Theoretically calculated dipole moment direction of (a) $ZnTPP(TPA)_2NO_2$ and (b) $ZnTPP(TPA)_2CHO$.

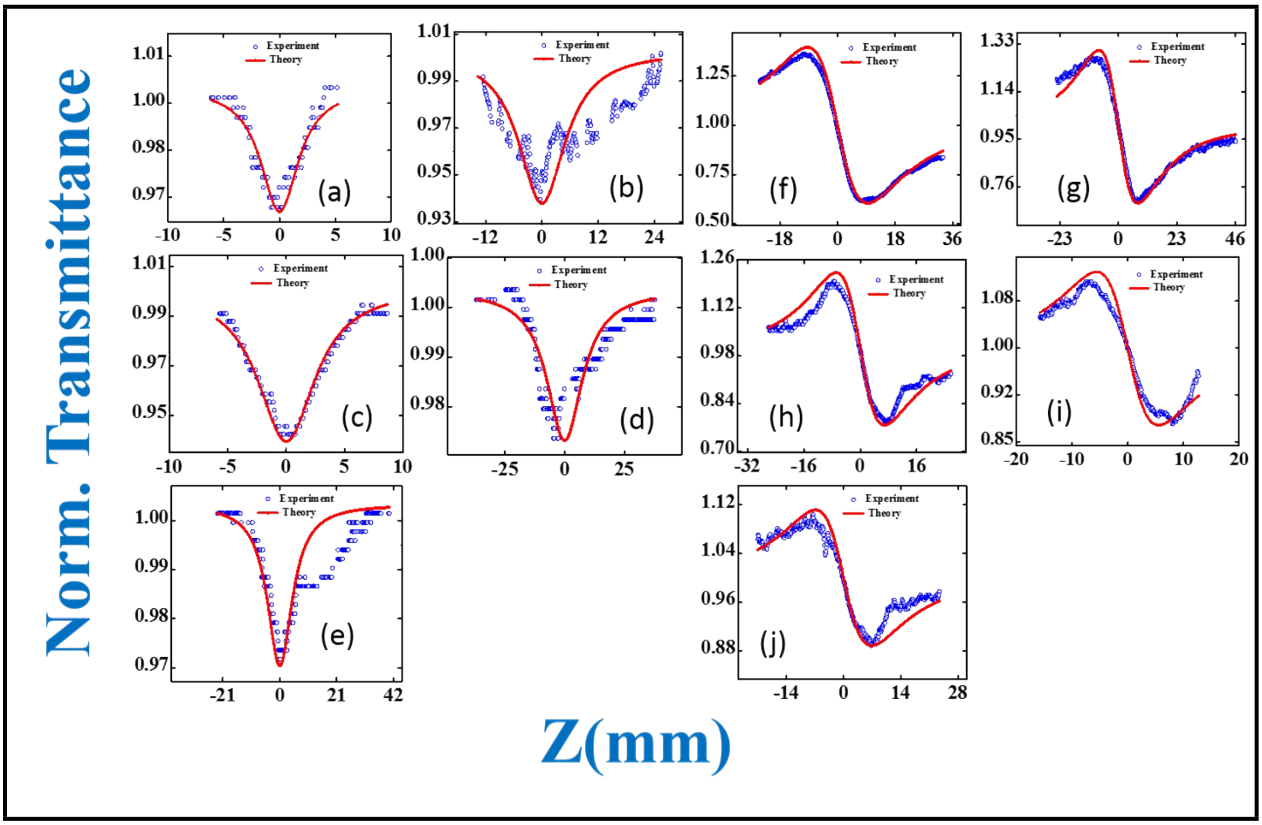

Figure S28: Experimental and theoretically fitted Z-scan data for sample **Zn(TPA)$_2$NO$_2$** in OA mode at (a) 680 nm (b) 700 nm (c) 750 nm (d) 800 nm (e) 850 nm and CA mode at (f) 680 nm (g) 700 nm (h) 750 nm (i) 800 nm (j) 850 nm. Open symbols are the experimental data points while the solid lines are the theoretical fits.

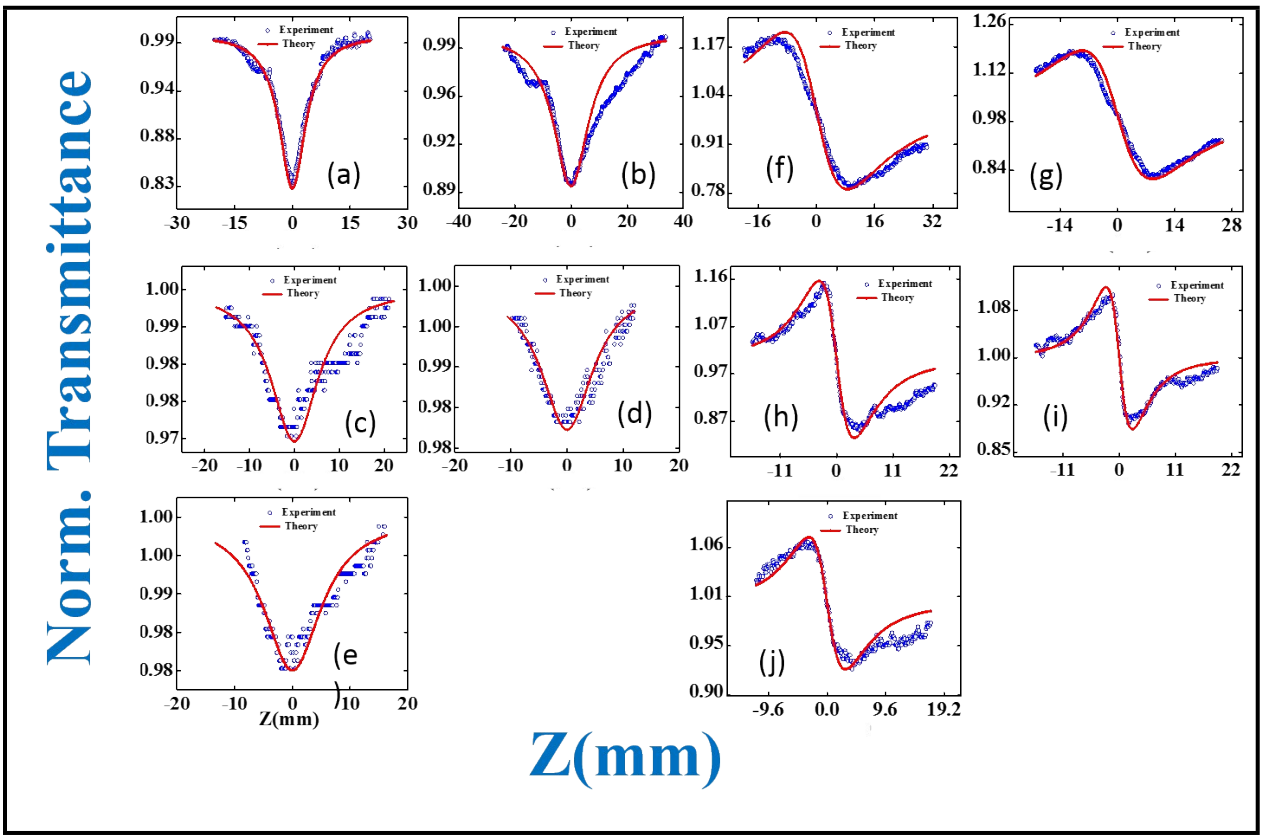

Figure S29: Experimental and theoretically fitted Z-scan data for sample **Zn(TPA)$_2$CHO** in OA mode at (a) 680 nm (b) 700 nm (c) 750 nm (d) 800 nm (e) 850 nm and CA mode at (f) 680 nm (g) 700 nm (h) 750 nm (i) 800 nm (j) 850 nm. Open symbols are the experimental data points while the solid lines are the theoretical fits.